

## SOME PHYSICAL PROPERTIES OF FTO/n-CdS/Au STRUCTURE

A. Ş AYBEK\*, H. RÜZGAR

*\*Department of Physics, Eskişehir Technical University, Eskişehir 26470, Turkey*

The cadmium sulfide film was obtained on the FTO glass substrate by chemical bath deposition technique. X-ray diffraction spectrum has revealed that the film was polycrystalline with cubic phase. The optical band gap of the film was evaluated from the absorbance measurement in the wavelength range 300-1800 nm. CdS film have direct band gap with the band gap value is 2.35 eV. The optical transmittance value of the film is %80 in the visible region. The curve of log I versus log V was seen space-charge-limited current regime. The capacitance-voltage (C-V) characteristics of FTO/n-CdS/Au structure have been measured at the various frequencies 100-500 kHz. The conductance-frequency characteristics of FTO/n-CdS/Au structure have been measured and the experimental result shows that the presence of the non-uniform distribution of the interface state. The crystal structural, optical and electrical properties of CdS film was carried out at the room temperature.

(Received October 12, 2018; Accepted November 28, 2018)

*Keywords:* CdS film, Chemical bath deposition, Space-charge-limited current

### 1. Introduction

II-VI compound semiconductors have shown a great advantage in various electronic devices and as optical windows for solar cells applications [1]. CdS films have an important role in applications such as light emitting diodes for flat panel displays, transistors for electronic switches and solar cells [2]. The CdS films have two crystal forms like the hexagonal close-packed (wurtzite), and the face-centred cubic (zinc blende or hawleyite). The CdS film shows *n*-type semiconduction properties due to sulphur deficiency [3, 4]. The CdS films have a high absorption coefficient and direct band gap material, and its optical band gap values are from 2.32 to 2.45 eV [5-7]. The highest efficiencies chemically deposited CdS semiconductor compounds have interesting properties for solar cells. CdS have been used as a window material in the highest efficiency thin film solar cells based on CdTe/CdS and (Cu (In, Ga) Se<sub>2</sub>) CIGS/ CdS films [8]. The optical and electrical properties of the CdS films depend strongly on the deposition techniques [9]. They have been prepared through different chemical and physical techniques like vacuum evaporation [9], sputtering [5], close-spaced sublimation [10], electrodeposition [11], molecular beam epitaxy [12], ultrasonic spray pyrolysis [6] and chemical bath deposition (CBD) [1, 13]. Among these, CBD has become the favoured route because of its simpleness, low temperature, reproducibility and inexpensive, large-area deposition technique for the CdS films. In the CBD process, the influence of the deposition parameters on the film formation, especially the quality and stoichiometry of the films differ as their structural and optical properties depend on the deposition conditions such as pH of the bath solution, deposition temperature and deposition time, etc. [1].

In this work, CdS film has been deposited onto fluorine tin oxide (FTO) substrate by the CBD method at 80 °C bath temperature to obtain the good and adherent film. The structural and optical properties of CdS film have been analyzed by XRD, UV-vis spectrometry. Also, we investigated some junction parameters of the structure by the electrical measurements such as; current-voltage, capacitance-voltage and conductance-frequency.

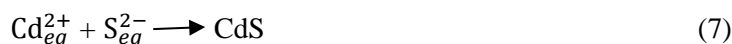
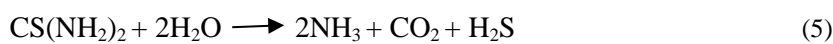
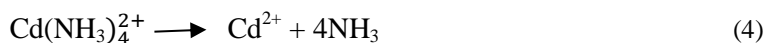
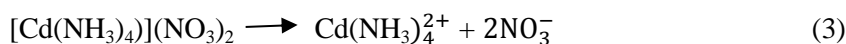
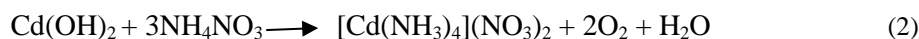
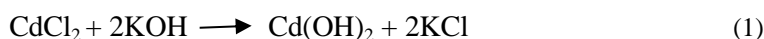
---

\* Corresponding author: saybek@anadolu.edu.tr

## 2. Experimental details

### 2.1. Deposition of the CdS film

The CdS semiconductor film was deposited on FTO-covered glass substrate by CBD technique. The glass substrate was cleaned by boiling in water with detergent about ten minutes and then rinsed with distilled water and dried by compressed air. The substrate was degreased by ultrasonic treatment in distilled water for about 15 minutes and dried by compressed air. Finally, it was etched in acetone and propane successively and then dried by compressed air. The bath solution of concentration 0.02 M was found to give good quality stoichiometry of CdS. Aqueous 0.02 M  $\text{CdCl}_2 \cdot \text{H}_2\text{O}$  and 0.2 M  $(\text{NH}_2)_2\text{CS}$  dissolved in deionized water, and 0.5 M KOH, 1.5 M  $\text{NH}_4\text{NO}_3$  were used to obtain CdS. The cleaned FTO glass substrate is dipped in the bath solution for 40 minutes at  $80^\circ\text{C}$ . The pH of the solution was maintained with the ammonia solution. The addition of ammonia solution slowly dropped into the bath solution to adjust the pH 10.40. The reaction of the CdS formation on the substrate can be given as:



After the deposition, the CdS film was washed softly in distilled water to remove the loosely adhered CdS particles on the film and finally dried in an oven at  $80^\circ\text{C}$  temperature. The deposited CBD-CdS film was seen homogenous, well adherent to the FTO-covered glass substrate and having a shiny. The growth of film was seen a better front side of the glass. The film on the back side of the substrate was removed by using nitric acid, while on the other side was used for all the measurements. The FTO/n-CdS/Au sandwich structure of the metal–semiconductor–metal system has been obtained by vacuum vapour deposition of the gold electrodes on the film. The space between gold and FTO electrodes was about 300 nm that it is the thickness of the CdS film and the area of the top electrode was about  $11 \text{ mm}^2$ . Copper wires were attached to the top and bottom electrodes by small droplets of silver paste. In this way, the FTO/n-CdS/Au sandwich structure was obtained. A schematic cross-section of the FTO/n-CdS/Au sandwich structure is shown in Fig. 1. The film was kept in dark before measurement. The film was found to be n-type as determined by the hot probe method.

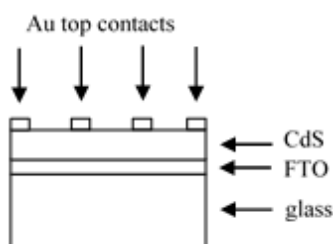


Fig. 1. A schematic cross-section of the FTO/n-CdS/Au sandwich structure.

## 2.2 Characterization of the CdS film

The phase and crystal structure investigation was found out by Bruker D8-X-Ray Diffractometer using  $\text{CuK}_\alpha$  radiation of  $\lambda=1.5406 \text{ \AA}$  in the detector scan mode, within the range of  $20^\circ\text{--}75^\circ$ . The optical absorbance and transmittance data of the film were carried out by SolidSpec-3700 UV-VIS-NIR Spectrophotometer within the range 300–1800 nm. The current–voltage measurement was studied in a dark medium by using Agilent 34401 Model Digital Multimeter, an HP 4140B pA meter/dc voltage source, and VEE One Lab 6.1 Computer program by applying silver contacts over the film and the results are presented. The capacitance–voltage and conductance–frequency characteristics were carried out with an HP 4192A LF impedance analyzer at room temperature and in the dark.

## 3. Results and discussions

### 3.1. Crystal structural properties of the CdS film on FTO substrate

Fig. 2 shows the X-ray diffraction pattern for CdS film deposited on FTO glass substrate. The XRD spectrum contains several peaks indicating that the films are polycrystalline in nature. The XRD reflections peaks are corresponding to the CdS cubic phase (JCPDS 01-089-0440) and FTO monoclinic phase (JCPDS 01-089-1727).

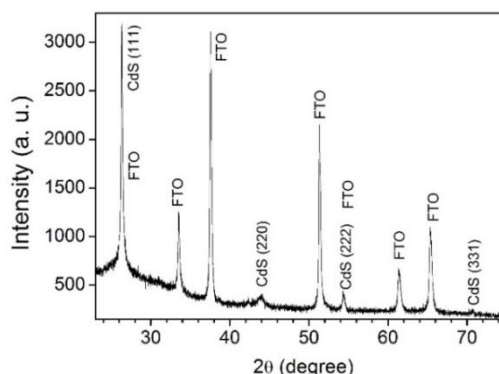


Fig. 2. X-ray diffraction spectrum of the CdS film on FTO substrate.

The cubic phase in CdS is commonly observed in as-grown layer by CBD technique [13–15]. Only the CdS peaks are found at  $44.15^\circ$  and  $70.65^\circ$ , and they correspond to (220) and (331) planes of face-centered cubic, respectively. It is thought that the other peaks take place both to CdS and FTO. Within the investigated range of parameters, no differences in the peak positions were observed. The (111) and (222) peaks of the cubic structure appear not clearly in the pattern, but the angle values corresponding to the peaks suitable for the data of JCPDS 01-089-0440.

### 3.2. Optical properties of the CdS film

UV–vis spectrometry has been employed to understand the optical properties of the prepared CBD-CdS film deposited on the FTO substrate. The absorption spectrum of the CdS film is shown in Fig. 3., recorded for wavelengths from 300 to 1800 nm. It is shown that a sharp rise in absorbance occurs between 450 and 530 nm wavelength. These regions are called fundamental absorption edges. The fundamental absorption refers to the valence band to the conduction band transition in n-type semiconductors. From the fundamental absorption can be used to determine the energy band gap of the semiconductor films [16]. The band gap of CdS film was evaluated by plotting graph between  $(ah\nu)^2$  against the photon energy ( $h\nu$ ), with help of the optical absorbance

spectrum. The optical band gap  $E_g$  is deduced using the Tauc relation. Tauc's relation is given by equation [17],

$$\alpha h\nu \approx (h\nu - E_g)^n \quad (8)$$

where  $\alpha$  is the absorption coefficient,  $h$  is the Planck constant and  $\nu$  is the frequency of incident photon on the CdS film.  $E_g$  is the energy difference between valence and conduction band of the film and  $n$  is equal to 1/2 for direct band transition gap material such as CdS [18] and 2 for indirect bandgap material. The absorption coefficient is about  $10^4 \text{ cm}^{-1}$ , deduced from the absorption spectrum, is also an indication of the direct transition [16]. The  $E_g$  value of CdS film is shown in Fig. 4 which is determined by the intercept of the straight line with the  $h\nu$  axis gives the  $E_g$ . The obtained band gap value is found to be 2.35 eV. This value is found to be in good agreement with those reported by Kumarage et al. [19]. They found that the optical band gap of CdS film prepared by CBD at the 80 °C is 2,34 eV. Also, reported [3], the value of 2.34 eV for the band gap was also determined to be the CdS/FTO film deposited by CBD. The transmittance spectrum is given in Fig. 5, which was recorded for wavelengths ranging from 300 to 1800 nm. Interference fringes are seen in the CdS film on deposited FTO. The optical transmission of deposited CdS film was 80% showed transmittance in the visible region.

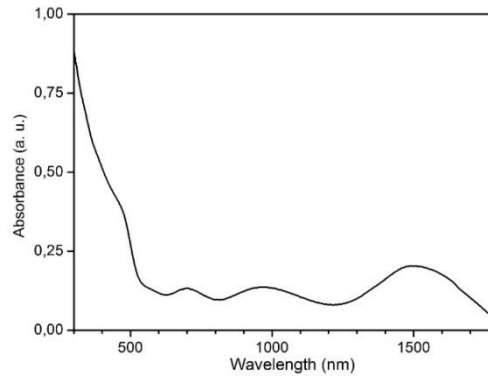


Fig. 3. Optical absorbance spectrum of CdS film.

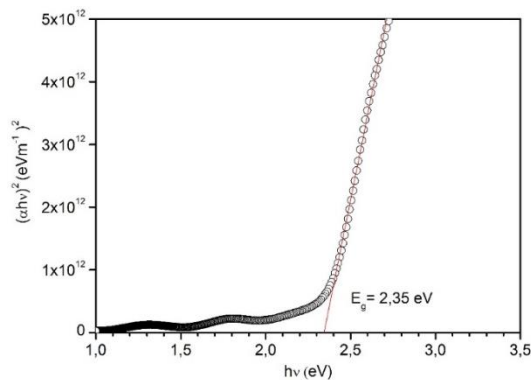


Fig. 4.  $(\alpha h\nu)^2$  versus photon energy ( $h\nu$ ) for the CdS film.

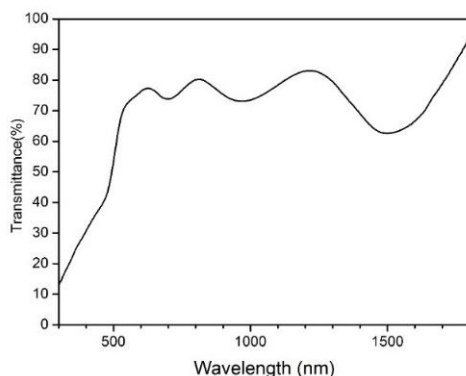


Fig. 5. Optical transmittance spectrum of CdS film.

### 3.3. Electrical properties of the CdS Film

Fig. 6 shows I-V characteristic of the FTO/n-CdS/Au structure was measured at different under forward bias of 0 - 1 V in the dark at room temperature. The measurements were done after keeping the FTO/n-CdS/Au structure in dark and at room temperature for one hour. In the electrical properties of the FTO/n-CdS/Au structure was studied by variation of a logarithm of current ( $\log I$ ) with the logarithm of voltage ( $\log V$ ). The curve of  $\log I$  versus  $\log V$  was plotted and analyzed using  $I/V^m$  relation. The  $\log I$ - $\log V$  characteristic allows us to understand some aspects of the charge carrier transport mechanism through FTO/n-CdS/Au structure. As can be seen from Fig. 6, the plot contains three conduction regions with a different slope. The region I shows an ohmic behaviour with a slope about unity. In this region, the dominant conduction mechanism is governed by Ohm's law at the lower voltages up to nearly 0.12V across the device. In region II, the current suddenly rise at  $V_{TFL}$  voltage where  $V_{TFL}$  is the trap-filled-limit (TFL) voltage, all the traps will become full and the current will rise rapidly by an amount  $\theta_o^{-1}$  where  $\theta_o$  is the ratio of free-to-trap charge. In region III, a trap-free region where the traps are filled. This means that the ohmic region follows trap-filled-limit region is known as trap states located below the Fermi level energy in the energy gap [20, 21].

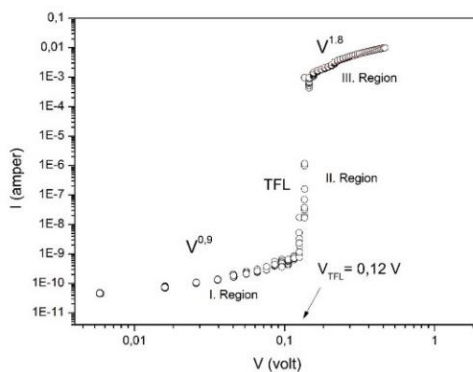


Fig. 6. The LogI-LogV characteristic of the FTO/n-CdS/Au structure.

In Fig. 7, we show the forward and reverse bias capacitance-voltage spectrum for FTO/n-CdS/Au structure in the frequency range 100 - 500 kHz. The values of capacitance increase with the decreasing frequency especially in depletion region due to interface state or interface traps.

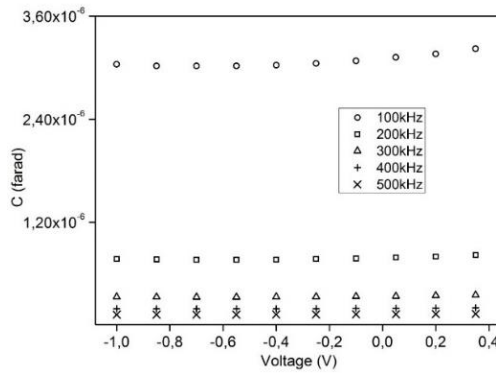


Fig. 7. The C-V dependence in both reverse and forward biasing at different frequencies for FTO/n-CdS/Au.

This occurs because at lower frequency interface state density can easily follow the ac signal and yield excess capacitance, which depends on the frequency at interface states or interface traps. [22-23] As can be seen from this expression the diffusion potential is usually determined by means of extrapolation of the linear  $C^{-2}$  versus  $V$  plot to the  $V$  axis,

$$C^{-2} = \frac{2}{\epsilon_0 \epsilon_s e A^2 N_d} (V_{bi} + V) \tag{9}$$

where  $V_{bi}$  is the built-in potential,  $e$  is the electron charge,  $A$  is the surface area of the interface,  $N_d$  is the density of the ionized traps like the donor,  $\epsilon_0$  and  $\epsilon_s$  are dielectric constant of the free space and the semiconductor, respectively. An interfacial layer can vary these characteristics if the potential across this layer changes with bias. In such a case, both the slope and the voltage axis intercept of the  $C^{-2} \sim V$  plot become functions of the interface layer thickness and the density of the interface states [24,25]. A nonlinear  $C^{-2} \sim V$  plot which is caused by the interface states can be transformed into a linear  $(C-C_0)^{-2} \sim V$  plot by determining the "excess capacitance"  $C_0$  which is the intercept of the  $C^{-2} \sim V$  in Fig.8. The slope of  $1/(C-C_0)^2$  versus  $V$  relationship of the obtained lines between -1 and -0.7 volts, where gives the  $N_d$  and  $V_{bi}$  obtained from the extrapolation intercept of  $1/(C-C_0)^2$  with the voltage axis. The obtained  $N_d$  and  $V_{bi}$  values are found to be  $6.33 \times 10^{15} \text{ cm}^{-3}$  and 0.43 V, respectively. For the value of  $N_d$  and  $V_{bi}$  are found to be  $1.2 \times 10^{17} \text{ cm}^{-3}$  and 0.4 V, respectively by Ref. [26].

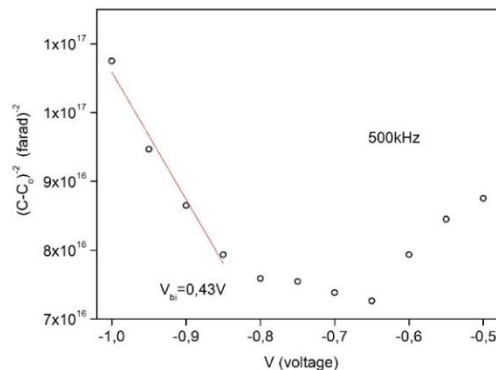


Fig. 8. The  $(C-C_0)^{-2} - V$  characteristic at 500 kHz for FTO/n-CdS/Au.

Fig. 9. shows conductance-frequency characteristics of the FTO/n-CdS/Au structure in the voltage range -1 – 0.4 V. From the figure the plots indicate a peak. These plots show that the conductance is dependent on the applied frequency.

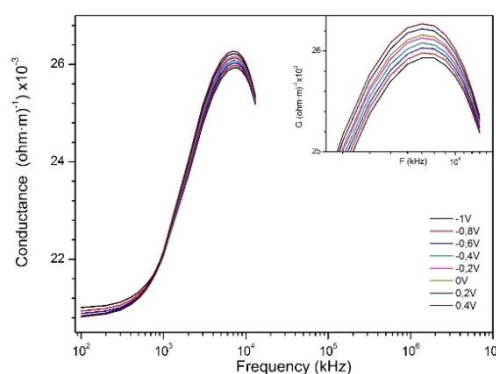


Fig. 9. The conductance versus frequency dependence at different voltages of FTO/n-CdS/Au.

The value of the conductance is increasing in forward bias till a point where it reaches a maximum value and decreasing after that. This increasing behaviour is attributed to the presence of the distribution of the interface state in the energy gap of CdS film. Furthermore, when we have carefully look at the inset in Fig 9, it is seen that the peak positions do not change to higher frequencies with the bias applied. This behaviour is attributed to the presence of a non-uniform distribution of the interface states inside the CdS film [27, 28].

#### 4. Conclusions

The crystal structure of CdS film is indicated that face centred cubic. The energy band gap value was found to be 2.35 eV. The CdS film exhibited also optical transmittance value 80% in the visible region. The space-charge-limited conduction mechanism is observed in the FTO/n-CdS/Au structure. The deep traps have been determined below the Fermi energy level in the energy gap. The built-in voltage and interface state density are found to be 0.43 V and  $6.33 \times 10^{15} \text{ cm}^{-3}$ , respectively. It is obtained that the traps show non-uniform distribution from the conductance-frequency characteristic.

#### References

- [1] L. Zhou, X. Hu, S. Wu, Surf. Coat. Technol. **228**, 171 (2013).
- [2] J.-H. Kwon, J.-S. Ahn, H. Yang, Curr. Appl. Phys. **13**, 84 (2013).
- [3] A. Zyoud, I. Saadeddin, S. Khudruj, Z. M. Hawash, D. Park, G. Campet, H. S. Hilal, Solid State Sci. **18**, 83 (2013).
- [4] Z. Pan, Y. Li, X. Hou, J. Yan, C. Wang, Physica E **63**, 1 (2014).
- [5] M. A. Islam, M. S. Hossain, M. M. Aliyu, P. Chelvanathan, Q. Huda, M. R. Karim, K. Sopian, N. Amin, Energy Procedia **33**, 203 (2013).
- [6] A. S. Aybek, M. Kul, E. Turan, M. Zor, E. Gedik, J. Phys.: Condens. Matter **20**, 055216 (2008).
- [7] L. Kong, J. Li, G. Chen, C. Zhu, W. Liu, J. Alloy. Compd. **573**, 112 (2013).
- [8] F. Liu, Y. Lai, J. Liu, B. Wang, S. Kuang, Z. Zhang, J. Li, Y. Liu, J. Alloy. Compd. **493**, 305 (2010).
- [9] J. Lee, Appl. Surf. Sci. **252**, 1398 (2005).
- [10] G. Pérez-Hernández, J. Pantoja-Enríquez, B. Escobar-Morales, D. Martínez-Hernández, L. L. Díaz-Flores, C. Ricardez-Jiménez, N. R. Mathews, X. Mathew, Thin Solid Films **535**, 154 (2013).
- [11] G. Sasikala, R. Dhanasekaran, C. Subramanian, Thin Solid Films **302**, 71 (1997).
- [12] S. Petillon, A. Dinger, M. Grün, M. Hetterich, V. Kazukauskas, C. Klingshirn, J. Liang, B. Weise, V. Wagner, J. Geurts, J. Cryst. Growth **201-202**, 453 (1999).

- [13] N. Maticiuc, J. Hiie, *Mater. Sci. Eng.* **49**, 012061 (2013).
- [14] S. Vatavu, C. Rotaru, V. Fedorov, T. A. Stein, M. Caraman, I. Evtodiev, C. Kelch, M. Kirsch, P. Chetruş, P. Gaşin, M. Ch. Lux-Steiner, M. Rusu, *Thin Solid Films* **535**, 244 (2013).
- [15] E. Yücel, O. Şahin, *Ceram. Int.* **42**, 6399 (2016).
- [16] J. I. Pankove, *Optical Processes in Semiconductors* (Prentice-Hall, Englewood Cliffs, NJ, 1971).
- [17] J. Tauc, *Mater. Res. Bull.* **3**, 37 (1968).
- [18] H. Khallaf, I. O. Oladeji, G. Chai, L. Chow, *Thin Solid Films* **516**, 7306 (2008).
- [19] W. G. C. Kumarage, L. B. D. R. P. Wijesundara, V. A. Seneviratne, C. P. Jayalath, B. S. Dassanayake, *Procedia Eng.* **139**, 64 (2016).
- [20] M. Lampert, *Current Injection in Solids*, Academic Press, New-York, 351 (1970).
- [21] M. Zor, C. A. Hogarth, *Phys.stat.sol. A* **99**, 513 (1987).
- [22] H. C. Card, E. H. Rhoderick, *J. Phys. D: Appl. Phys.* **4**, 1589 (1971).
- [23] S. Kar, W. E. Dahlke, *Solid State Electron.* **15**, 869 (1972).
- [24] S. J. Fonash, *J. Appl. Phys.* **54**, 1966 (1983).
- [25] E. H. Rhoderick, R. H. Williams, *Metal-Semiconductor Contacts*. 2nd Ed. (Clarendon, Oxford, 1988).
- [26] N. B. Chaure, S. Bordas, A. P. Samantilleke, S. N. Chaure, J. Haigh, I. M. Dharmadasa, *Thin Solid Films* **437**, 10 (2003).
- [27] F. Yakuphanoglu, *Sensor Actuat. A: Phys. A* **147**, 104 (2008).
- [28] S. S. Fouad, G. B. Sakr, I. S. Yahia, D. M. Abdel-Basset, F. Yakuphanoglu, *Mater. Res. Bull.* **49**, 369 (2014).